Journal of Applied Mechanics Vol.12, pp.383-394 (August 2009) JSCE

Rationale for coefficient of earth pressure at rest derived from prismatic sand heap

Thirapong PIPATPONGSA*, Sokbil HENG**, Atsushi IIZUKA*** and Hideki OHTA****

* Member, Doctor of Engineering, Assoc. Prof., Global Scientific Information and Computing Center,
** Member, Master of Engineering, Doctoral student, Dept. of International Development Engineering,
Tokyo Institute of Technology (2-12-1 O-okayama, Meguro-ku, Tokyo 152-8550)
***Member, Doctor of Engineering, Professor, Research Center for Urban Safety and Security
Kobe University (1-1 Rokkodai-cho, Nada-ku, Kobe 657-8501)
****Member, Doctor of Engineering, Professor, Research and Development Initiative
Chuo University (1-13-27 Kasuga, Bunkyo-ku, Tokyo 112-8551)

The semi-empirical relationship between coefficient of earth pressure at rest K_o and the internal friction angle proposed by Jáky is widely accepted in practice. This relationship is a simplified equation derived from the stress state in a prismatic sand heap inclined at the angle of repose on the rough and firm base. Though Jáky's derivation is theoretically correct, it was later considered coincidence. This study examined other possible derivations of the relationship based on Jáky's approach by using scaled stress and generalized shear stress reduction functions. The results of formulation lead to associate lateral stress ratio in the center of sand heap with degree of arching. The analyzed stress distribution, in which the major compressive stresses carry the granular weight to the base in a particular pattern, is found reliable with experimental data and indicates a good agreement with Jáky's K_o expression.

Key Words: *coefficient of earth pressure at rest, elasto-plasticity, arching, granular media, numerical analysis*

1. Introduction

The coefficient of earth pressure at rest, K_o, is the ratio of effective horizontal pressure to vertical pressure, acting on principal planes in the condition of horizontally constrained deformation. Analyses of many geotechnical engineering problems often require the magnitude of K_o to describe in-situ lateral earth pressure. Jáky (1944)[1)] initially derived the relationship between K_o and the internal friction angle ϕ as shown in Eq.(1). Later, Jáky (1948)[2)] simplified his original equation to Eq.(2) as the semi-empirical relationship. It is clear that both K_o equations reasonably provide $K_a<K_o<1$ where K_a is a coefficient of active earth pressure shown in Eq.(3). K_o obtained from Eq.(1) gives value about 90% of Eq.(2) over a range of ϕ between 10°-40°. Due to this small difference, the formula K_o=1-sinφ is well-known for geotechnical engineers due to its simplicity in practice, e.g. giving K_o = 1/2 whereas K_a = 1/3 for ϕ=30°.

$$K_o = \left(1+\frac{2}{3}\sin\phi\right)\frac{1-\sin\phi}{1+\sin\phi} \approx 0.9\left(1-\sin\phi\right) \tag{1}$$

$$K_o = 1-\sin\phi,\ K_a = \frac{1-\sin\phi}{1+\sin\phi} \qquad (2),\ (3)$$

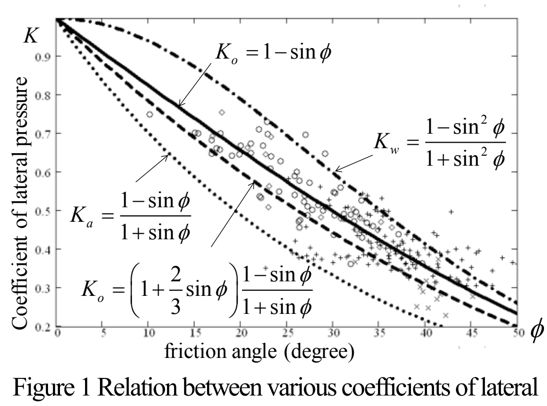

Figure 1 Relation between various coefficients of lateral pressure and friction angle with some experimental data

Many researchers have been studied and determined magnitudes of K_o from in-situ and laboratory tests for a world-wide variety of soils[3)-7)]. Despite of discussions on the influences of stress history, stress level, void ratio, inhomogeneous degree and effect of ϕ based on either peak or residual shear strength, those of researches arrive to a common conclusion that, the measured values for homogeneous sands and clays in a state of primary loading show a good agreement with Jáky's correlation as shown in Fig. 1. Therefore, the attractive simplicity of Jáky's semi-empirical formula linking K_o to ϕ is widely accepted.

Much effort has been made to measure K_o because K_o is determined by strain-controlled, not a parameter obtained by stress-controlled experiment. It is doubted whether how this complicated relationship can be uniquely expressed in very simple terms, using only one basic soil parameter but applicable to almost soil types. Therefore, the Jáky's formula from the theoretical standpoint has drawn many interests. Though formulation of Jáky's K_o is not familiar due to disadvantage to publishing in Hungarian, Jáky's assumption and analytical method were critically examined[6),8)-11)]. It was found that,

(i) The analysis is not associated with one-dimensional strain state but the result of principal stress orientation regulated by the particularly assumed shear stress distribution in granular mound.

(ii) The boundary condition does not correspond to K_o physical condition of a wide loaded area where horizontal boundary of soil mass is infinite; therefore, the validity of Jáky's K_o equation should be exclusively applied to the center line of symmetrical embankments with slope forming the angle of repose with the horizontal ground surface.

In earlier research, a ratio between lateral to vertical pressures at the symmetry axis of a wedge was assumed constant and termed as a compaction factor K in Brahtz (1936)'s solution of stress distribution[12)]. In the same context, Jáky (1944)[1)] formulated the K_o equation from a stress analysis in a long wedge-shaped granular heap in loose state lying at the angle of repose ϕ as depicted in Fig. 2. The coefficient of lateral stress K at the symmetrical line of the mound, whose elastic region is sandwiched by plastic region, was considered to be K_o. In-plane purely frictional Coulomb material with fixed slip planes in plastic region was assumed while the shear stress distribution was supposedly reduced to zero at the center in elastic region.

Michalowski (2005)[11)] pointed out that Jáky's analytical method proposed in 1944 is theoretically acceptable. But stress distribution across the width of the heap was found unrealistic when comparing to the experiments on sand piles, e.g. Vanel et al. (1999)[13)]. This verification leads to the conclusion that Jáky's K_o is a coincidental findings (see also Handy[9)], 1985) which happens to fit with laboratory measurements.

In fact, the resemble hypothesis used in Jáky (1944)[1)] was considered to explain the curious phenomenon of central pressure dip underneath the granular mound (Wittmer et al., 1996, 1997)[14)-15)]. Cantelaube & Goddard (1997)[16)], Cates et al. (1998)[17)] and Didwania et al. (2000)[18)] also analyzed the stress distribution in granular wedge by separating the continuum into elastic and plastic regions. All stress components satisfying the stress equilibrium were continuously across this boundary (see Figs. 2-3). The analytical solutions reveal the vertical normal stress at the center can exhibit a dip, a peak and a flat by varying the adjustable parameter which is a value of the slope separating the elastic-plastic boundary. The closure remarked the variation of vertical pressure is caused by arching action over the base of the heap. A case of pressure dip surprisingly gives a coefficient of lateral stress K at the mid-plane of the heap equal to 1 while a case of flat distribution of vertical pressure gives K equal to K_w which is known as Krynine (1945)'s wall coefficient[19)]. K_w is defined as the ratio of the lateral to vertical stress mobilized along a vertical plane. It is clear that K_w gives higher value than Jáky's K_o, e.g. K_w=3/5 for ϕ=30°.

$$K_w = \frac{1}{1+2\tan^2\phi} = \frac{\cos^2\phi}{1+\sin^2\phi} = \frac{1-\sin^2\phi}{1+\sin^2\phi} \tag{4}$$

Therefore, the magnitude of K involves a certain degree of arching and there is a particular arching criterion which can associate with K_o. However, the relation of stress distribution with arching action in sand heap is remaining unclear. The authors have reviewed Jáky's approaches on stress analyses in sand heap and storage silo (Heng et al., 2008)[20)]. It is apparent that Jáky assumed quadratic shear stress reduction in sand heap but differently assumed linear shear stress reduction in storage silo. There is no rational clue for these inconsistent assumptions.

This research aims to clarify the drawback of Jáky's basic assumption and examine other formulations of K_o by using a method of scaled stress with generalized shear stress reduction functions. In extension to the past researches, the authors consider the essence of Handy's arching assumption[9)] (1985) to widen Jáky's assumption in effort to validate K_o in prismatic sand heap. The resulted stress distribution is compared with the published experimental data. Interpretation of the results relating to arching effects is presented and discussed. This basic study is expected to be a useful review and rationale for theoretical validation of Jáky's semi-empirical K_o equation.

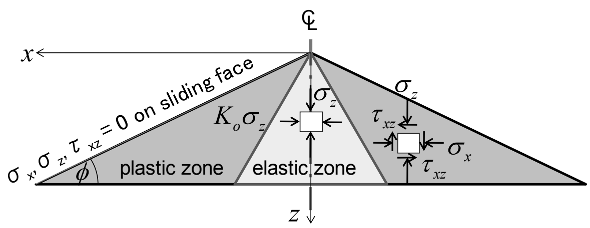

Figure 2 Prismatic sand heap lying at the angle of repose ϕ with the horizontal on a rigid and rough base. State of stress along the center line is considered as at-rest condition by Jáky (1944)

2. Theoretical Background

According to the review made by Savage (1998) [21], analysis and modelling of stress distribution under either prismatic or conical heaps have been extensively studied, ranging from Airy's stress function approach in earth dam[12], discrete approach in embankment[22)-23], continuum approach in sand piles[10)-11),14)-17),24] and recently by finite element method[25]. Despite of numerous techniques, this study focuses on the continuum approach for prismatic heap in an attempt to present the analytical method that conforms to Jáky's approach.

2.1 Continuum Mechanics Approach

A sand heap can be assumed to be a homogeneous body because a length scale of a whole material is sufficiently large in compare with individual sizes of particles. A sand heap, which is composed of numbers of granules, can be symmetrically piled up on rough and firm surface in a long prismatic shape with the highest slope inclined at the angle of repose ϕ. Self weight transferred to vertical support stabilizes the sliding force due to the frictional resistance among sand particles and along surface roughness of the base.

As illustrated in Fig. 3, due to a symmetrical shape, the half width of the heap ACO is considered, where the vertical z-axis is measured vertically downwards from the apex of the mound and the horizontal x-axis is measured horizontally outwards. The slope OA is inclined with horizontal AC at the reposed angle ϕ. The internal friction angle ϕ is generally equivalent to the angle of repose for loose deposit of granular materials.

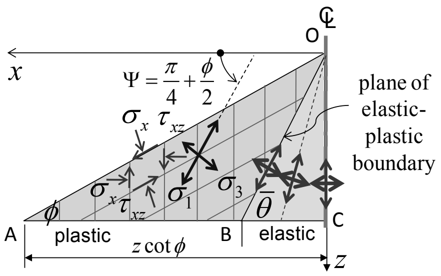

Figure 3 Idealized plastic and elastic regions in half-width body. Elastic core is sandwiched by plastic crusts along the plane of elastic-plastic boundary sloping at angle $\bar{\theta}$. It is considered $\bar{\theta} \leq \Psi$ where Ψ represents the direction of the maximum compressive stress in plastic region.

In Fig.3, the continuum of the mound is divided into plastic and elastic regions by the plane OB. The outer plastic shells are slipped along layers of infinite slope. We can see that the whole plastic crust ABO is placed above the inner region of elastic core BCO. Blocks of finite thickness in ABO are sliced by two sets of slip planes; the parallel plane to the slope surface and the vertical plane. Stress components along the elastic-plastic boundary must be connected. Therefore the continuum of stress is maintained along the slope OB oriented at the angle $\bar{\theta}$ from the horizontal. We can observe that the elastic core is symmetrical along OC plane. This plane is assumed by Jáky as the plane of at-rest condition where the direction of major principal stress is normal to the base. At the free-surface AO, material is essentially in a zero stress state. Moreover, at the mid-plane OC, shear stress must be zero due to symmetry and absence of frictional horizontal support. Stress components throughout the heap must satisfy the two-dimensional equilibrium equations condition given below,

$$\begin{Bmatrix} \dfrac{\partial \sigma_x}{\partial x} + \dfrac{\partial \tau_{xz}}{\partial z} \\ \dfrac{\partial \tau_{xz}}{\partial x} + \dfrac{\partial \sigma_z}{\partial z} \end{Bmatrix} = \begin{Bmatrix} 0 \\ \gamma \end{Bmatrix} \tag{5}$$

where σ_x is a horizontal stress, σ_z is a vertical stress, τ_{xz} is a shear stress, γ is a unit weight of bulk material. The subscript x and z refer to horizontal and vertical axes as depicted in Figs.2-3.

2.2 Scaled Stress Functions

As a granular heap grows in size, the bulk material deposited in thin layers on the slope face remains inclined at the angle of repose. So there is no change in shape throughout the formation. By ignoring the bin effect, it is possible to find the similarity solution in which the stress states are proportionally increased with depth. Many research works assumes the patterns of stress distributed in granular heap are independent of height[10),14)-18),24),28]. By following Sokolovskii's scaled stress analysis of planar wedge[24], the ratios of stresses σ_x, σ_z and σ_{xz} to the equivalent geo-static pressure γz are respectively defined to the scaled stress variables χ_x, χ_z and χ_{xz}.

$$\chi_x = \sigma_x / \gamma z\,,\quad \chi_z = \sigma_z / \gamma z\,,\quad \chi_{xz} = \tau_{xz} / \gamma z \qquad (6), (7), (8)$$

According to Eqs.(6)-(8), we can substitute $\sigma_x = \gamma z \chi_x$, $\sigma_z = \gamma z \chi_z$ and $\sigma_{xz} = \gamma z \chi_{xz}$ to Eq.(5) and arrive to Eq.(9).

$$\begin{Bmatrix} \dfrac{\partial \chi_x}{\partial x} + \dfrac{\partial \chi_{xz}}{\partial z} \\ \dfrac{\partial \chi_{xz}}{\partial x} + \dfrac{\partial \chi_z}{\partial z} \end{Bmatrix} = \frac{1}{z} \begin{Bmatrix} -\chi_{xz} \\ 1 - \chi_z \end{Bmatrix} \tag{9}$$

Under the scaled stress analysis, similar patterns of stress distributions are assumed to all depth. That means the scaled stress variables are depended only on a scaling variable x/z. By adapting Wittmer's notation[15], a relative width s is defined in Eq.(10) as a scaling variable x/z normalized by the maximum value at the slope face. Fig. 4 envisages a geometrical transformation of a heap from a physical scale (in dimension of height H and half-width of base $H\cot\phi$) to a normalized scale. We note that s=0 at the symmetrical line passing the center, s=1 at the slope face and $s = \bar{s}$ at the elastic-plastic boundary. We can see that $\bar{s}$ does not only mark the elastic-plastic boundary described by Eq.(11), but $\bar{s}$ can be also regarded as a proportion of elastic zone in a body of a heap.

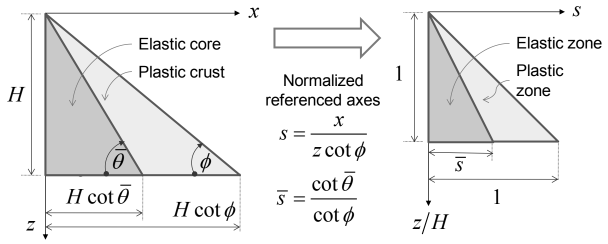

Figure 4 Normalized geometry of granular heap from a physical geometry (left) to a scaled geometry (right)

$$s=\frac{x}{z\cot\phi},\quad \overline{s}=\frac{\cot\overline{\theta}}{\cot\phi} \tag{10), (11}$$

According to Eq.(10), spatial derivatives of s with respect to coordinates x and z are given by the following equations.

$$\frac{\partial s}{\partial x}=\frac{1}{z\cot\phi},\quad \frac{\partial s}{\partial z}=-\frac{s}{z} \tag{12), (13}$$

As mentioned earlier, stress field function $\sigma_x(x,z)=\gamma z\chi_x(x/z)$, $\sigma_z(x,z)=\gamma z\chi_z(x/z)$ and $\sigma_{xz}(x,z)=\gamma z\chi_{xz}(x/z)$ are basically postulated in Sokolovskii's scaled stress analyses of wedge[24]. For convenience, the scaled stress variables are modeled to be a function of a relative width s in this study as described in Eqs.(14)-(16). The derivatives of χ_x, χ_z and χ_{xz} with respect to s are given by Eqs.(17)-(22).

$$\chi_x=\chi_x(s),\quad \chi_z=\chi_z(s),\quad \chi_{xz}=\chi_{xz}(s) \tag{14),(15),(16}$$

$$\frac{\partial\chi_x}{\partial x}=\frac{\partial\chi_x}{\partial s}\frac{\partial s}{\partial x},\quad \frac{\partial\chi_x}{\partial z}=\frac{\partial\chi_x}{\partial s}\frac{\partial s}{\partial z} \tag{17), (18}$$

$$\frac{\partial\chi_z}{\partial x}=\frac{\partial\chi_z}{\partial s}\frac{\partial s}{\partial x},\quad \frac{\partial\chi_z}{\partial z}=\frac{\partial\chi_z}{\partial s}\frac{\partial s}{\partial z} \tag{19), (20}$$

$$\frac{\partial\chi_{xz}}{\partial x}=\frac{\partial\chi_{xz}}{\partial s}\frac{\partial s}{\partial x},\quad \frac{\partial\chi_{xz}}{\partial z}=\frac{\partial\chi_{xz}}{\partial s}\frac{\partial s}{\partial z} \tag{21), (22}$$

The system of ordinary differential equations in terms of scaled stress variables and relative width can be formulated by substitutions of Eqs.(14)-(22) to Eq.(9).

$$\begin{bmatrix}\dfrac{\partial s}{\partial x} & 0\\ 0 & \dfrac{\partial s}{\partial z}\end{bmatrix}\cdot\begin{Bmatrix}\dfrac{\partial\chi_x}{\partial s}\\ \dfrac{\partial\chi_z}{\partial s}\end{Bmatrix}+\frac{\partial\chi_{xz}}{\partial s}\begin{Bmatrix}\dfrac{\partial s}{\partial z}\\ \dfrac{\partial s}{\partial x}\end{Bmatrix}=\frac{1}{z}\begin{Bmatrix}-\chi_{xz}\\ 1-\chi_z\end{Bmatrix} \tag{23}$$

Three unknown variables in Eq.(23) are χ_x, χ_z and χ_{xz} while number of equations are two, therefore one additional equation is necessary to solve the system of equations. This required equation is usually regarded as a class of constitutive equation in continuum mechanics.

Providing that a particular form of χ_{xz} is known, the derivatives $\partial\chi_x/\partial s$ and $\partial\chi_z/\partial s$ can be solved from the above differential equation.

$$\frac{\partial\chi_x}{\partial s}=\cot\phi\left(s\frac{\partial\chi_{xz}}{\partial s}-\chi_{xz}\right) \tag{24}$$

$$\frac{\partial\chi_z}{\partial s}=\frac{\tan\phi\dfrac{\partial\chi_{xz}}{\partial s}+\chi_z-1}{s} \tag{25}$$

The integral forms of above differential equations $\chi_x(s)$ and $\chi_z(s)$ can be manipulated below.

$$\chi_x=\int\cot\phi\left(s\frac{\partial\chi_{xz}}{\partial s}-\chi_{xz}\right)ds+c_x \tag{26}$$

$$\begin{aligned}\chi_z&=\frac{\displaystyle\int\frac{\tan\phi\dfrac{\partial\chi_{xz}}{\partial s}-1}{s}e^{\int\frac{-1}{s}ds}ds+c_z}{e^{\int\frac{-1}{s}ds}}\\&=\left(\int\frac{1}{s^2}\left(\tan\phi\frac{\partial\chi_{xz}}{\partial s}-1\right)ds+c_z\right)s\end{aligned} \tag{27}$$

The integral constants c_x and c_z are obtained from the boundary conditions. The necessary boundary conditions are given at the continuity of state of stresses along the slope boundary $\overline{s}$ which separates plastic and elastic regions.

$$\overline{\chi}_x=\chi_x(\overline{s}),\quad \overline{\chi}_z=\chi_z(\overline{s}) \tag{28), (29}$$

By using the described boundary conditions Eqs.(28)-(29) to Eqs.(26)-(27), the algebraic solution of χ_x and χ_z can be expressed.

$$\chi_x=\overline{\chi}_x+\int_{\overline{s}}^{s}\cot\phi\left(s\frac{\partial\chi_{xz}}{\partial s}-\chi_{xz}\right)ds \tag{30}$$

$$\chi_z=\left(\frac{\overline{\chi}_z}{\overline{s}}+\int_{\overline{s}}^{s}\frac{1}{s^2}\left(\tan\phi\frac{\partial\chi_{xz}}{\partial s}-1\right)ds\right)s \tag{31}$$

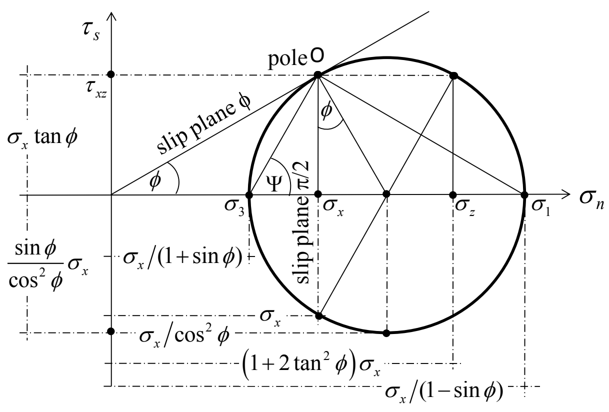

Figure 5 Typical Mohr stress circle used to describe the state of stresses in fully mobilized plastic zone of a granular heap inclined at angle of repose. Pole O is determined by the intersection of a slip plane ϕ of slope face and a conjugate slip plane π/2. The angle Ψ indicates the direction of major principal stress. By geometry, $\Psi=\pi/4+\phi/2$ inclined with the horizontal

3. Local Constitutive Equations

The constitutive equation of materials is generally expressed in stress invariants and independent of boundary condition. However, closures in several papers proposed local constitutive equations to explain stress distribution in sand heap (see Savage, 1998)[21]. This study is also restricted to the local constitutive equation because the specific boundary condition is embedded. Throughout this study, components of normalized stress are given by the following conditional expressions which obey two local constitutive equations used in plastic ("*p*" superscript) and elastic ("*e*" superscript) regions.

$$\chi(s)=\begin{cases}\chi^{p}(s) & \text{if } s\geq\bar{s}\\ \chi^{e}(s) & \text{otherwise}\end{cases} \tag{32}$$

3.1. Mohr-Coulomb Criterion with Fixed Principal Axes

In plastic region, stress in bulk material is characterized by the Mohr-Coulomb failure criterion with zero cohesion. In this closure, the slip planes are fixed, the angle of major principal direction is $\Psi=\pi/4+\phi/2$. The states of stresses described by Mohr's stress circle exhibited in Fig.5, are expressed as follow.

$$\tau_{xz}=\sigma_x\tan\phi\text{, thus }\chi^{p}_{xz}=\chi^{p}_{x}\tan\phi \tag{33}$$

$$\sigma_z=\sigma_x+2\tau_{xz}\tan\phi\text{, thus }\chi^{p}_{z}=\left(1+2\tan^2\phi\right)\chi^{p}_{x} \tag{34}$$

From Eq.(33) and Eq.(34), the derivatives of χ^p_{xz} and χ^p_z with respect to s are obtained.

$$\frac{\partial\chi^{p}_{xz}}{\partial s}=\tan\phi\frac{\partial\chi^{p}_{x}}{\partial s}\ ,\ \frac{\partial\chi^{p}_{z}}{\partial s}=\left(1+2\tan^2\phi\right)\frac{\partial\chi^{p}_{x}}{\partial s} \tag{35), (36}$$

Substitutions of Eqs.(33), (35) to Eq.(24) and Eqs. (34), (35) to Eq.(25) can obtain the following derivatives with respect to s.

$$\frac{\partial\chi^{p}_{x}}{\partial s}=s\frac{\partial\chi^{p}_{x}}{\partial s}-\chi^{p}_{x}\text{, thus }\frac{\partial\chi^{p}_{x}}{\partial s}=\frac{-\chi^{p}_{x}}{1-s} \tag{37}$$

$$\frac{\partial\chi^{p}_{z}}{\partial s}=\frac{\tan^2\phi\dfrac{\partial\chi^{p}_{x}}{\partial s}+\left(1+2\tan^2\phi\right)\chi^{p}_{x}-1}{s} \tag{38}$$

Combining Eqs.(36)-(38) can derive the solutions given below.

$$\chi^{p}_{x}(s)=\left(1-s\right)\cos^2\phi \tag{39}$$

$$\chi^{p}_{z}(s)=\left(1-s\right)\left(1+\sin^2\phi\right) \tag{40}$$

$$\chi^{p}_{xz}(s)=\left(1-s\right)\sin\phi\cos\phi \tag{41}$$

Since the continuity of all stresses on boundary between elastic and plastic zones marked on $\bar{s}$ is required. Components of boundary stresses variables are expressed by substitution of $s=\bar{s}$ into Eqs.(39)-(41).

$$\bar{\chi}_x=\chi^{p}_{x}(\bar{s})\ ,\ \bar{\chi}_z=\chi^{p}_{z}(\bar{s})\ ,\ \bar{\chi}_{xz}=\chi^{p}_{xz}(\bar{s}) \tag{42), (43), (44}$$

3.2 Shear Stress Reduction Models

Central core behaves elastically, so the state of stresses lies inside Mohr-Coulomb failure criterion. The local constitutive equations in elastic region are generalized and explained. The possible solutions can be derived under shear stress reduction models which appeared in Witter et al. (1996, 1997)[14)-15)]. It was later extended and verified by Catelaube and Goddard (1997)[16)], Cates et al. (1998)[17)] and Didwania et al. (2000)[18)]. This class of closure assumes that shear stress in elastic core is linearly reduced along horizontal distant from elastic-plastic boundary to zero at the center. To include non-linearity in this study, the extended shear stress reduction models are suggested in form,

$$\chi^{e}_{xz}=r(\eta,a,b)\bar{\chi}_{xz} \tag{45}$$

where $\eta=s/\bar{s}\in[0,1]$ is an internal coordinate, $r\in[0,1]$ is a non-linear reduction function and $\bar{s}$ marks the elastic-plastic boundary. The simple form of r functioned with η can be characterized by the following curving function,

$$\left(1-\eta\right)^{a}+r^{b}=1\text{, hence }r(\eta,a,b)=\left(1-\left(1-\eta\right)^{a}\right)^{1/b} \tag{46}$$

where a and b are positive real numbers which help adjust an desired curvature. The derivatives of χ^e_{xz} with respect to a normalized slope s can be given by,

$$\begin{aligned}\frac{\partial\chi^{e}_{xz}}{\partial s}&=\frac{\partial r}{\partial\eta}\frac{\partial\eta}{\partial s}\bar{\chi}_{xz}\\&=\frac{a}{b}\left(1-\frac{s}{\bar{s}}\right)^{a-1}\left(1-\left(1-\frac{s}{\bar{s}}\right)^{a}\right)^{\frac{1-b}{b}}\frac{\bar{\chi}_{xz}}{\bar{s}}\end{aligned} \tag{47}$$

where $\dfrac{\partial r}{\partial\eta}=\dfrac{a}{b}\left(1-\eta\right)^{a-1}r^{1-b}$, $\dfrac{\partial\eta}{\partial s}=\dfrac{1}{\bar{s}}$ by Eqs.(45)-(46).

It is remarked that $\partial\chi^e_{xz}/\partial s$ (or $\partial r/\partial\eta$) is undefined at s=0 (or η=0) for b>1. Nevertheless, 5 cases of reduction function are studied and illustrated in Fig.6, including the case of b>1 employed in case (3). Using Eqs.(45)-(47) together with Eqs.(30)-(31), the solution of stress profiles can be obtained for each shear reduction models. Detailed solutions are grouped in Appendix case (1) to case (5). A coefficient of lateral earth pressure K at the center of granular heap can be evaluated as a ratio of the horizontal stress to vertical stress. K is determined by a limit of σ_x/σ_z when s approaches to 0 as shown below.

$$K=\lim_{s\to 0}\frac{\sigma_x}{\sigma_z}=\lim_{s\to 0}\frac{\chi^{e}_{x}}{\chi^{e}_{z}}\quad\text{due to Eqs.(6)-(7)} \tag{48}$$

In linear reduction model (see Appendix case (1)), for a given $\bar{s}$, χ^e_x maintains constant, χ^e_z is linearly dependent on s. This solution is confirmed with the earlier research (Cantelaube & Goddard, 1997)[16)]. Despite of undefined K in case (3), according to the expressions of K summarized in Table 1, it can be concluded that K are depended on a choice of reduction functions and $\bar{s}$ is considered as an adjustable parameter.

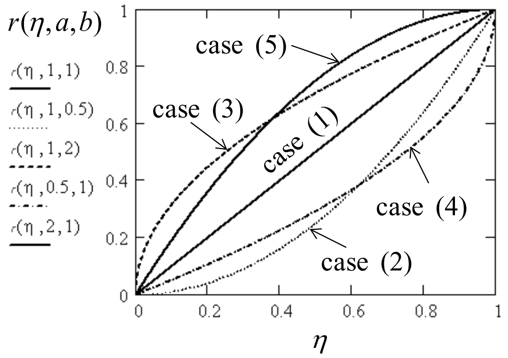

Figure 6 Various variations of reduction functions

Table 1 Coefficients of lateral pressure K expressed as functions of elastic-plastic boundary slope in corresponding to 5 selected cases of shear stress reduction.

Cases	$\chi_{xz}^{e}/\bar{\chi}_{xz}$	$K(\bar{s})=\lim_{s\to 0}\dfrac{\chi_x^e}{\chi_z^e}$
(1)	$\dfrac{s}{\bar{s}}$	$\dfrac{\bar{s}\left(1-\bar{s}\right)\cos^2\phi}{\bar{s}-\left(1-\bar{s}\right)\sin^2\phi}$
(2)	$\left(\dfrac{s}{\bar{s}}\right)^2$	$\left(1-\dfrac{\bar{s}}{3}\right)\left(1-\bar{s}\right)\cos^2\phi$
(3)	$\left(\dfrac{s}{\bar{s}}\right)^{1/2}$	undefined
(4)	$1-\left(1-\dfrac{s}{\bar{s}}\right)^{1/2}$	$\dfrac{2\left(1-\dfrac{\bar{s}}{3}\right)\left(1-\bar{s}\right)\bar{s}\cos^2\phi}{2\bar{s}-\left(1-\bar{s}\right)\sin^2\phi}$
(5)	$1-\left(1-\dfrac{s}{\bar{s}}\right)^2$	$\dfrac{\left(1+\dfrac{\bar{s}}{3}\right)\left(1-\bar{s}\right)\bar{s}\cos^2\phi}{\bar{s}-2\left(1-\bar{s}\right)\sin^2\phi}$

3.3 Jáky's assumption

In regarding to Fig.3, the direction of major principal stress inclines at Ψ and the direction of elastic-plastic boundary inclines at $\bar{\theta}$ with horizontal. Jáky (1944)[1] particularly chose $\bar{\theta}$ equal to Ψ in order to prohibit shear stress along elastic-plastic boundary. Therefore, $\bar{s}$ can be determined from Eqs.(49)-(50), consequently the solutions for stress distribution can be solved and demonstrated in Figs.7-11 for ϕ=33°.

In linear reduction of case (1) is known as "FPA model" (fixed principal axis) coined by Wittmer et al. (1996, 1997)[14)-15)] because Ψ is fixed throughout the mound. Michalowski (2005)[11)] emphasized that Wittmer's assumption appears to resemble the theoretical effort of Jáky by choosing $\bar{\theta}=\Psi$.

$$\Psi=\frac{\pi}{4}+\frac{\phi}{2},\quad \bar{s}=\frac{\cot\bar{\theta}}{\cot\phi}=\frac{\cot\Psi}{\cot\phi}=\frac{\sin\phi}{1+\sin\phi} \qquad (49),\ (50)$$

FPA model associates to the extreme case of arching effect due to the central stress dip. Wittmer et al. (1996)[14)] explained that the uniform stack of arches carrying self weight to the base lies straight with constant direction. It is surprised that an isotropic condition is achieved at the center line because K=1.

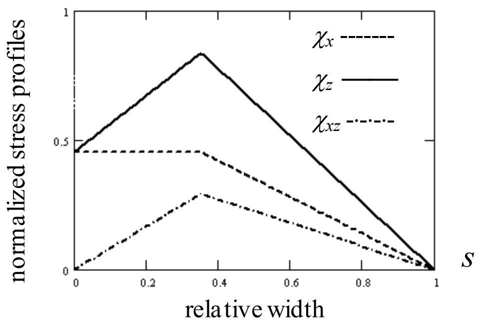

Figure 7 Resulted stress distribution by shear reduction case (1)

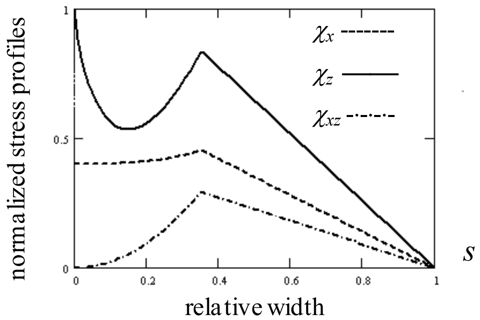

Figure 8 Resulted stress distribution by shear reduction case (2)

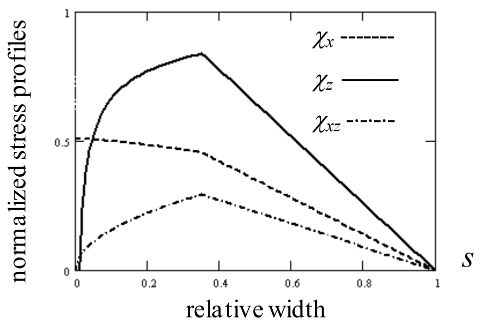

Figure 9 Resulted stress distribution by shear reduction case (3)

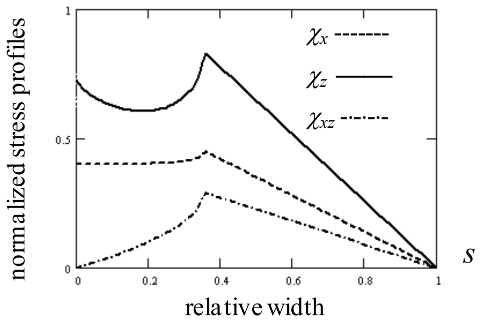

Figure 10 Resulted stress distribution by shear reduction case (4)

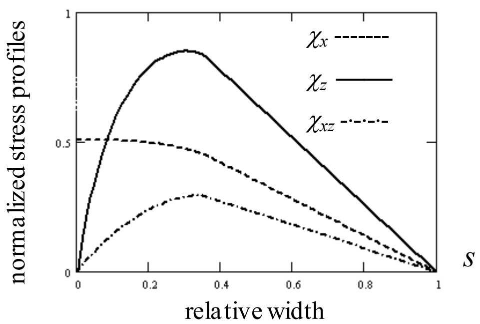

Figure 11 Resulted stress distribution by shear reduction case (5)

In effort to formulate K_o equation, Jáky (1944) proposed quadratic reduction of shear stress[1)] (see Appendix case (2)) as given in Eq.(71) Manipulations of equations to obtain the solution are explained shortly (see details in Michalowski, 2005)[11)]. The expression of Jáky (1944)'s K_o is obtained thru K in Eq.(75), derived by integration of partial derivatives obtained in Eq.(72) with the boundary conditions defined in Eqs.(42) -(43), using $\bar{s}$ specified in Eq.(50). The resulted stress profiles are demonstrated in Fig.8. But the vertical stress profile with local minimum appearance is considered unreliable by Michalowski (2005)[11)] when comparing with typical experimental results.

In a similar manner, to formulate other possible K equations which can be derived by the condition between case (1) and case (2), more detailed derivations are added in this study by power rules as given in Eq.(76) in Appendix case (2.1): a=1, b=1/(1+n). A positive number $n \geq 0$ is applicable in regard to the applicable range discussed previously that $0<b\leq 1$ should be used in reduction functions to avoid singularity. The formulation of K in this case is shown in Eq.(51). It is found that there are two distinct conditions of K for n=0 and n>0.

$$K = \begin{cases} 1 & \text{if} \quad n=0 \\ \dfrac{1+\dfrac{2}{2+n}\sin\phi}{1+\sin\phi}\left(1-\sin\phi\right) & \text{if} \quad n>0 \end{cases} \tag{51}$$

Table 2 shows variation of K by various n. It is found that as $n\rightarrow 0$, $K\rightarrow 1-\sin\phi$ is exactly the expression of K_o used in Jáky (1948)[2)]. But if n=0, K=1. To explain the reason of immediate change, the stress profiles for various n are plotted in Fig.12. It can be see that the vertical stress $\sigma_z=\gamma z$ at the center equals to geo-static pressure when n>0 but $\sigma_z=\gamma z(1-\sin\phi)$ when n=0.

Therefore, formulations of K for case (1)-(5) are theoretically correct but the resulted stress fields appear unrealistic due to an inappropriate adjustable parameter. Condition of Eq.(50) adopted in Jáky's assumption unreasonably equates the slope of elastic-plastic boundary to the major compressive direction.

Table 2 Influence of power degree to coefficient of lateral earth pressure based on nonlinear reduction of shear stress

n	K	Note
∞	$\dfrac{1-\sin\phi}{1+\sin\phi}$	Rankine's active ratio
1	$\left(1+\dfrac{2}{3}\sin\phi\right)\dfrac{1-\sin\phi}{1+\sin\phi}$	Jáky (1944)[1)]
1/2	$\left(1+\dfrac{4}{5}\sin\phi\right)\dfrac{1-\sin\phi}{1+\sin\phi}$	
1/4	$\left(1+\dfrac{8}{9}\sin\phi\right)\dfrac{1-\sin\phi}{1+\sin\phi}$	
$1/\infty$	$1-\sin\phi$	Jáky (1948)[2)]
0	1	Wittmer et al. (1996)[14)]

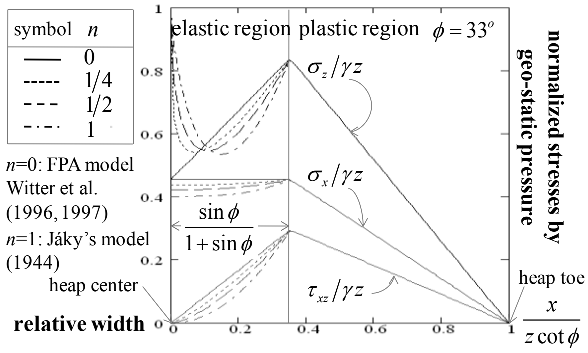

Figure 12 Unrealistic stress distribution results based on Jáky's assumption with the singularity at the center line of heap

4. Validation with Experimental Data

4.1 Experimental Data

The earliest measurements of normal stresses across the base of a granular wedge were conducted by Hummel and Finnan (1920)[26)], following by a series of sand wedge experiments carried out by Trollope (1957)[22)] and Lee and Herington (1971)[27)]. It is of interest that an intuitive expectation in considering the maximum amount of pressure underneath a poured sand heap is sensed commonly in the middle, directly under the apex. But in fact, the results of experiments have been reported that a granular media exerts its maximum pressure at a slight distant from the centre point depends upon 2D/3D geometry, rigidity/deflection of the base and the formation process/construction history of the heap.

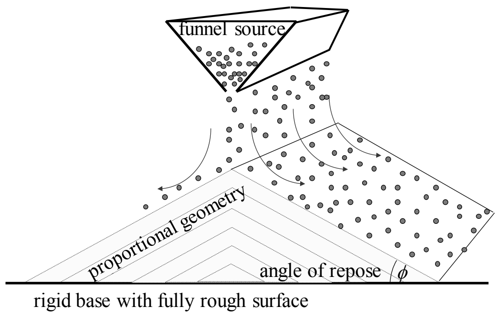

Figure 13 Heap constructed by pouring sand from a funnel source in sequences of prismatic wedge

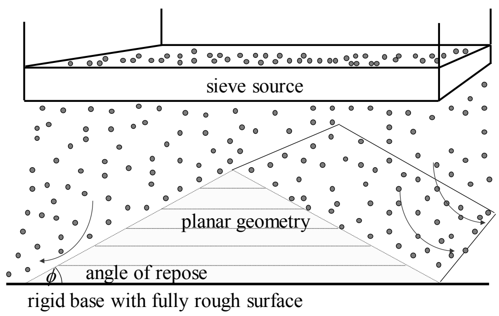

Figure 14 Heap constructed by pouring sand from a sieve source in sequences of raining layer

This fact was systematically confirmed by experiments of Vanel et al. (1999)[13] on poured sand of ϕ=33°. A series of experiments on sand heap using two different sand dispensing sources; funnel source and sieve source is referred in this study. During deposition processes, the pouring sources were moved upward to control the density of deposition. The heap grows in a proportional geometry under the funnel source (see Fig. 13) while spreading in a planar layer under the sieve source (see Fig. 14). The heap constructed by the sieve source rarely exhibited a central pressure dip, but obviously occurred by the funnel source for both 2D wedge-shaped and 3D conical heaps with weaker effect on wedge-shaped heap.

4.2 Analytical Results

Though, there are experimental data reported for both conical and prismatic heaps, conical heaps are out of scope in this study. In the context of prismatic wedge, the solutions given in case (1) and case (5) are further considered by dropping case (3) due to singularity problem at the centerline, and cases (2) and (4) due to unrealistic local minimum in vertical stress profiles. In case (1), if $\bar{s}$ is selected in the way to keep χ^{e}_{z} constant, then the solutions are reduced to those obtained by Bouchaud, Cates & Claudin (1995)[28]. This solution is termed "BCC model" and can explain that the stacks of arches rotate in elastic region under uniform vertical stress distribution. Actually, this solution resembles Trollope (1957)'s no arching solution[22]. The expression of K turns to Krynine (1945)'s wall coefficient K_w[19]. According to case (1), $\bar{s}$ is related to K as follows.

$$\bar{s} = \frac{1 - \dfrac{1+\sin^2\phi}{1-\sin^2\phi}K + \sqrt{\left(1-K\right)^2 + \left(2K\sin\phi/\cos^2\phi\right)^2}}{2} \tag{52}$$

Obviously, various stress distribution can be obtained by varying the adjustable parameter $\bar{s}$, not necessary to be fixed like Jáky's assumption[1)-2)]. Because various lateral stress ratios K can be related to $\bar{s}$ in according to the formulations shown Table 1, K is correspondingly considered as adjustable parameter being varied with influence and history of heap formation. 4 different stress distributions are illustrated in Figs.15 for linear reduction model of case (1) and Fig.16 for non-linear reduction model of case (2), in accordance with 4 typical K values; K_a for active condition determined by Eq.(3), K_w for rough wall condition determined by Eq.(4), K_o for at-rest condition determined by Eq.(2) and K_i for isotropic condition by taking K=1.

Because arching action steers weight away from the center of sand heap, the transition from no-arching state when K=K_w to full-arching state when K=K_i is clearly observed in the analyzed vertical pressures exhibited in Fig.15 for linear shear reduction model. Moreover, for non-linear shear reduction model, the stress dip in the analyzed stress profiles exhibited in Fig.16 can be visibly captured for K<K_a. Non-linear shear reduction model is apparently more advantageous than linear shear reduction model by providing smoother stress profiles with arching indicatives. In general, both Fig.15 and Fig.16 indicate that vertical pressure dip is achieved for large value of K, resulting in large horizontal pressure and high shear stress profile along the base of the wedge.

The measurements on horizontal and shear stresses were not available in experiments of Vanel et al. (1999)[13]. Though sand heaps are rested on a base by a relative degree of arching effect depended on construction method, it is likely that the analyzed stress profile under K=K_o at the center of both models are acceptable agreed with averaged results of experimental data in prismatic heaps. However, K equation in at-rest condition of the heap cannot be derived without specifying $\bar{s}$ and degree of non-linearity which are unknown parameters for shear reduction models. Therefore, arching action might give a clue to formulate K_o equation.

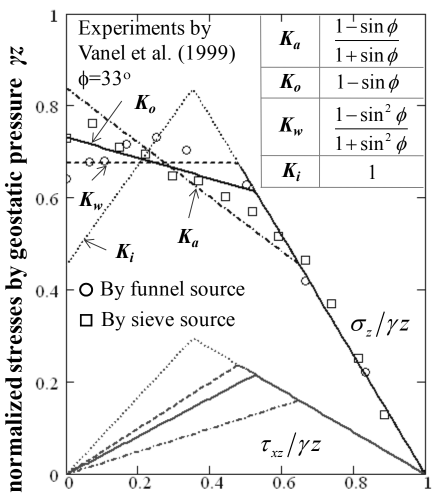

Figure 15 Normalized vertical pressure and shear stress profiles analyzed by linear shear reduction model

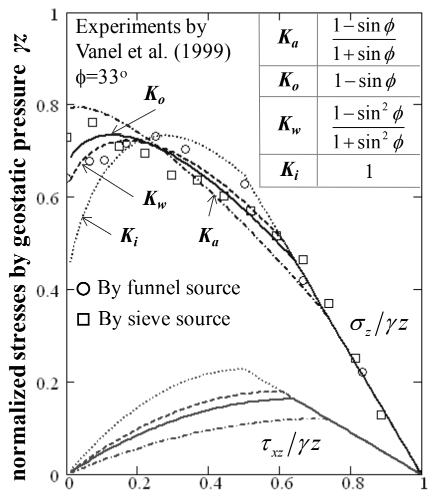

Figure 16 Normalized vertical pressure and shear stress profiles analyzed by non-linear shear reduction model

5. Arching Effect

Arching action is regarded as internal stress redistribution in granular media. Experimental results reported several cases of active arching in loose soils, which has upward shear stresses acting to soil mass. According to Handy (1985)[9], arching action can be formed in bulk materials along the trajectories of principal stresses to carry its own weight. Consequently, a concept of arch can be applied to evaluate earth pressure in stockpiles, silos, slopes, buried conduits and retaining walls.

5.1 Soil Arching

In sand heap, the granular arches can be regarded as chains of particles transferring self-weight to the base, and stacks of arches acted along the major compressive stresses dominate pressure distribution. Handy (1985)[9] suggested a shape of granular arch along the minor compressive stress is catenary like a hanging flexible chain acted by self-weight.

In regard to arching theory, Handy (1985)[9] purported that the expression K_o=1-sinϕ of Eq.(2) can be approximated by a flat arch partially supported by friction at the ends which is analogous to a parallel fully rough wall problem in which Jáky(1948)[2] initiated his semi-empirical K_o equation to analyse earth pressure in silo.

5.2 Arching Criterion

The flat arch in sand heap explained by Handy (1985) in an attempt to validate Jáky's (1948) K_o is not rigorously correct because the arch axis is not thoroughly fixed with the horizontal but rotated along the direction of principal stresses. Herein, a particular arching action is found to validate Jáky's (1948) K_o.

An arching criterion is assumed thru a distribution of the major principal stress σ_1 in the elastic core of the mound. Expressions of σ_1 and χ_1 are basically described by,

$$\sigma_1 = \frac{\sigma_x + \sigma_z}{2} + \sqrt{\left(\frac{\sigma_x - \sigma_z}{2}\right)^2 + \tau_{xz}^2} \tag{53}$$

$$\chi_1 = \frac{\sigma_1}{\gamma z} = \frac{\chi_x + \chi_z}{2} + \sqrt{\left(\frac{\chi_x - \chi_z}{2}\right)^2 + \chi_{xz}^2} \tag{54}$$

For a given depth, stack of arches loaded by its own weigh transfer constant $\bar{\sigma}_1$ ($\bar{\chi}_1$ in normalized or scaleed quantity) over the base in different direction from the plane of elastic-plastic boundary to the vertical plane at the center. Therefore, the scaled major compressive stress χ^e_1 is assumed to uniformly distribute over the elastic crust of the heap.

$$\chi_1^e = \bar{\chi}_1 \quad \text{where} \quad \bar{\chi}_1 = \chi_1^p(\bar{s}) \tag{55}$$

To keep the stress continuity, χ^e_1 must equal to χ^p_1 along the elastic-plastic boundary $\bar{s}$. Referring to Eq.(54), stresses in plastic crust obtained from Eqs.(39)-(41) results as follows.

$$\begin{aligned}\bar{\chi}_1 &= \frac{\chi_x^p(s) + \chi_z^p(s)}{2} + \sqrt{\left(\frac{\chi_x^p(s) - \chi_z^p(s)}{2}\right)^2 + \chi_{xz}^p(s)^2} \\ &= \left(1+\sin\phi\right)\left(1-\bar{s}\right)\end{aligned} \tag{56}$$

The expressions of χ^e_1 in terms of three stress components can be similarly expressed by referring to Eq.(54).

$$\chi_1^e = \frac{\chi_x^e + \chi_x^e}{2} + \sqrt{\left(\frac{\chi_x^e - \chi_x^e}{2}\right)^2 + \left(\chi_{xz}^e\right)^2} \tag{57}$$

We can relate χ^e_{xz} to χ^e_x and χ^e_z by substitution of Eq.(57) to Eq.(55). With minor rearrangement, a local constitutive equation for this particular condition can be manipulated.

$$\chi_{xz}^e = \chi_{xz}^e(s) = \sqrt{\left(\bar{\chi}_1 - \chi_x^e(s)\right)\left(\bar{\chi}_1 - \chi_z^e(s)\right)} \tag{58}$$

The derivatives of χ^e_{xz} with respect to s can be obtained from Eq.(58) using chain's rule of differentiation.

$$\frac{\partial \chi_{xz}^e}{\partial s} = \frac{\partial \chi_{xz}^e}{\partial \chi_x^e}\frac{\partial \chi_x^e}{\partial s} + \frac{\partial \chi_{xz}^e}{\partial \chi_z^e}\frac{\partial \chi_z^e}{\partial s} \tag{59}$$

According to Eq.(58), the partial derivatives of χ^e_{xz} with respect to χ^e_x and χ^e_z are given below.

$$\frac{\partial \chi_{xz}^e}{\partial \chi_x^e} = -\frac{\bar{\chi}_1 - \chi_z^e}{2\chi_{xz}^e}, \quad \frac{\partial \chi_{xz}^e}{\partial \chi_z^e} = -\frac{\bar{\chi}_1 - \chi_x^e}{2\chi_{xz}^e} \tag{60), (61}$$

Using the condition of equilibrium given by Eqs.(24)-(25), the derivatives of $\partial\chi^e_x/\partial s$ and $\partial\chi^e_z/\partial s$ can be obtained with some rearrangement in according to Eq.(59).

$$\frac{\partial \chi_x^e}{\partial s} = \frac{\left(1 - \chi_z^e - \dfrac{\chi_{xz}^e}{s\cot\phi}\right)\dfrac{\partial \chi_{xz}^e}{\partial \chi_z^e} + \chi_{xz}^e - \dfrac{\partial \chi_{xz}}{\partial s}s}{\dfrac{1}{\cot^2\phi}\dfrac{\partial \chi_{xz}^e}{\partial \chi_z^e} - \dfrac{s}{\cot\phi} + s^2\dfrac{\partial \chi_{xz}^e}{\partial \chi_x^e}}s \tag{62}$$

$$\frac{\partial \chi_z^e}{\partial s} = \frac{\dfrac{1-\chi_z^e}{\cot\phi} - \dfrac{\frac{\partial \chi_{xz}^e}{\partial s}}{\cot^2\phi} - \left(1 - \chi_z^e - \dfrac{\chi_{xz}^e}{s\cot\phi}\right)\dfrac{\partial \chi_{xz}^e}{\partial \chi_x^e}s}{\dfrac{1}{\cot^2\phi}\dfrac{\partial \chi_{xz}^e}{\partial \chi_z^e} - \dfrac{s}{\cot\phi} + s^2\dfrac{\partial \chi_{xz}^e}{\partial \chi_x^e}} \tag{63}$$

Stress continuity conditions at the elastic-plastic boundary $\bar{s}$ provide the boundary conditions to integrate the above differential equations. Since the analytical solution is complicated, we conducted a numerical solution using Runge-Kutta method. Some numerical techniques can be found in Pipatpongsa et al. (2008)[29]. The magnitude of $\bar{s}$ must be trialed until the condition of zero shear stress imposed on the center line where s=0 is satisfied. Consequently, for a given friction angle ϕ, the coefficient of lateral pressure K was obtained by calculating the ratio of χ^e_x/χ^e_z at the center line.

$$K(\phi) = \frac{\chi_x^e(0)}{\chi_z^e(0)} \quad \text{where} \quad \chi_{xz}^e(0) = 0 \tag{64}$$

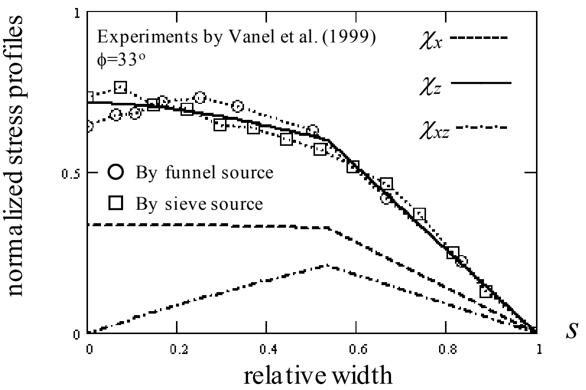

Figure 17 Resulted stress distribution by constant major compressive stress across the width of elastic crust

To validate the proposed assumption, the systematic experimental conducted by Vanel et al. (1999)[13)] was compared with calculated results. Though the solution gives a vertical pressure profile with no stress dip, Fig.17 shows that the measured data of vertical pressure agreed well with numerical solution. Also, according to Fig. 18, K values were found close to K_o=1-sinϕ which is the expression of Jáky (1948)[2)]. So, the proposed assumption on arching criterion in prismatic sand heap might be sufficiently capable to demonstrate the arching effect in the mound and validate the rationale of Jáky's K_o equation.

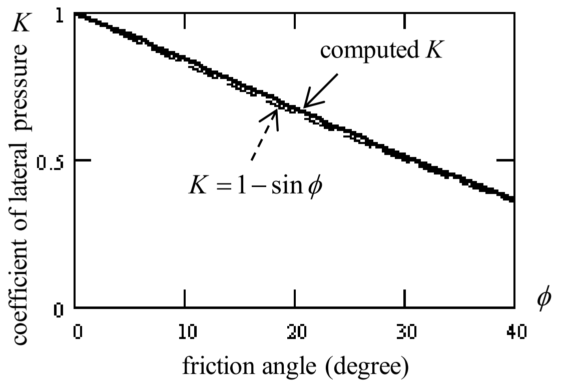

Figure 18 Comparison between the computed K and Jáky's K_o (1948) in relation with friction angle ϕ

Though the closed-form integration of the coupled system of partial differential equations cannot be analytically derived in this study, numerical integration of over a range of ϕ between 10° to 40° can estimate the expression of K to Eq.(65), which is approximately 2% larger than Jáky (1948)'s K_o.

$$K \approx 1.02(1 - \sin\phi) \tag{65}$$

The assumption of constant compressive stress distribution in elastic crust looks promising. Still, there are other possible arching criteria which can be assumed and investigated in prismatic sand heaps.

6. Conclusion

The value of K_o assumed by Jáky is the ratio of horizontal to vertical pressure at the center line of a granular formed by angle of repose. A series of stress solutions aiming to formulate K_o equations based on Jáky's hypothesis in prismatic granular mounds was reviewed and examined. The generalized shear stress reduction function was proposed and employed to local constitutive models for describing stress profiles in elastic zone of the heap. The implementation of scaled stress function, which is formulated in terms of dimensionless quantity of stress components normalized by the equivalent geo-static pressure, was proven to conveniently handle the partial differentiation with respect to the relative width of the half-based heap.

Stress profiles were derived by integration of the derivatives of equilibrium equations with the boundary conditions of zero stress at sliding surface as well as the stress continuity specified at elastic-plastic boundary. The results of this study confirmed the conclusion made in the earlier research that Jáky's K_o is a coincidental finding. The problem on adopting the slope of elastic-plastic boundary equal to the inclination of the major principal stress was clarified as the ambiguity in Jáky's hypothesis. The shear stress reduction model is still regarded as a general model among other possible models. Therefore, it is doubted why Jáky particularly chose a quadratic reduction model from a plenty number of models which can be used.

It was found the model of shear stress reduction cannot provide the coefficient of lateral pressure. So, it is understood that K_o is an adjustable parameter to fit the model with the experimental data. Nevertheless, degree of non-linearity of shear stress reduction was found to link with arching indicatives.

The analyzed stress distribution by the arching criterion, in which the major compressive stresses carry granular weight to the base in a particular pattern, is found reasonable. Constant distribution of the major compressive stress along elastic core underneath the wedge-shaped granular heap was presented as one of possible arching criteria. The validation of the suggested arching criterion showed that the calculated vertical pressure was matched with experimental results and coefficient of lateral earth pressure was considerably agreed with the widely-used K_o expression of Jáky (1948).

In this closure, the assumption of soil arching appears to rationally relate K_o with friction angle of granular media. Still, there is no clear model which can describe stress distribution in granular wedge because the self-weight transfer characteristics in the granular wedge are considered as elastic behaviors. As a result, elastic parameters should be relevant to K_o in addition to a friction angle. The suggested arching criterion is merely considered as a demonstrated model which can be assumed to justify the K_o expression of Jáky. More researches in arching criteria and arch shapes are required for further investigations.

Appendix

Case (1): $r(\eta,1,1)=\eta$

$$\chi_{xz}^{e}=\frac{s}{\overline{s}}\overline{\chi}_{xz}^{p},\ \frac{\partial\chi_{xz}^{e}}{\partial s}=\frac{\overline{\chi}_{xz}}{\overline{s}}=\frac{1-\overline{s}}{\overline{s}}\sin\phi\cos\phi \qquad (66),\ (67)$$

$$\chi_{x}^{e}=\left(1-\overline{s}\right)\cos^{2}\phi \qquad (68)$$

$$\chi_{z}^{e}=1-s-\left(1-\overline{s}\right)\left(\frac{\sin\phi}{\overline{s}}\right)^{2}\left(\overline{s}-\left(1+\overline{s}\right)s\right) \qquad (69)$$

$$K=\lim_{s\to0}\frac{\chi_{x}^{e}}{\chi_{z}^{e}}=\frac{\overline{s}\left(1-\overline{s}\right)\cos^{2}\phi}{\overline{s}-\left(1-\overline{s}\right)\sin^{2}\phi} \qquad (70)$$

Case (2): $r(\eta,1,1/2)=\eta^{2}$

$$\chi_{xz}^{e}=\left(\frac{s}{\overline{s}}\right)^{2}\overline{\chi}_{xz},\ \frac{\partial\chi_{xz}^{e}}{\partial s}=\frac{2s}{\overline{s}}\frac{\overline{\chi}_{xz}}{\overline{s}} \qquad (71),\ (72)$$

$$\chi_{x}^{e}=\left(1-\overline{s}\right)\left(1-\left(1-\left(\frac{s}{\overline{s}}\right)^{3}\right)\frac{\overline{s}}{3}\right)\cos^{2}\phi \qquad (73)$$

$$\chi_{z}^{e}=1-s+2s\left(1-\overline{s}\right)\left(\frac{\sin\phi}{\overline{s}}\right)^{2}\left(\frac{\overline{s}}{2}+\ln\left(\frac{s}{\overline{s}}\right)\right) \qquad (74)$$

$$K=\lim_{s\to0}\frac{\chi_{x}^{e}}{\chi_{z}^{e}}=\left(1-\frac{\overline{s}}{3}\right)\left(1-\overline{s}\right)\cos^{2}\phi \qquad (75)$$

Case (2.1): $r\left(\eta,1,\frac{1}{1+n}\right)=\eta^{1+n}$ for $0>n>1$

$$\chi_{xz}^{e}=\left(\frac{s}{\overline{s}}\right)^{1+n}\overline{\chi}_{xz},\ \frac{\partial\chi_{xz}^{e}}{\partial s}=\left(1+n\right)\left(\frac{s}{\overline{s}}\right)^{n}\frac{\overline{\chi}_{xz}}{\overline{s}} \qquad (76),\ (77)$$

$$\chi_{x}^{e}=\left(1-\overline{s}\right)\left(1-\frac{n\overline{s}}{2+n}\left(1-\left(\frac{s}{\overline{s}}\right)^{2+n}\right)\right)\cos^{2}\phi \qquad (78)$$

$$\chi_{z}^{e}=1-\left(s+\left(s+\frac{\left(\frac{s}{\overline{s}}\right)-\left(\frac{s}{\overline{s}}\right)^{n}}{\frac{1-n}{1+n}}\right)\left(1-\frac{1}{\overline{s}}\right)\sin^{2}\phi\right) \qquad (79)$$

$$K=\lim_{s\to0}\frac{\chi_{x}^{e}}{\chi_{z}^{e}}=\left(1-\frac{n}{2+n}\overline{s}\right)\left(1-\overline{s}\right)\cos^{2}\phi \qquad (80)$$

Note: it is found that Eq.(80) is reduced to Eq.(75) for n=1 in regardless of the singularity in Eq.(79). However, Eq.(80) is not reduced to Eq.(70) for n=0. Therefore, the expression of K in case (2.a) can cover case (2), but cannot cover case (1).

Case (3): $r(\eta,1,2)=\eta^{1/2}$

$$\chi_{xz}^{e}=\left(s/\overline{s}\right)^{1/2}\overline{\chi}_{xz},\ \frac{\partial\chi_{xz}^{e}}{\partial s}=\frac{1}{2}\left(\frac{s}{\overline{s}}\right)^{-1/2}\frac{\overline{\chi}_{xz}}{\overline{s}} \qquad (81),\ (82)$$

$$\chi_{x}^{e}=\left(1-\overline{s}\right)\left(1+\frac{1-\left(s/\overline{s}\right)^{3/2}}{3}\right)\cos^{2}\phi \qquad (83)$$

$$\chi_{z}^{e}=1-s-\frac{1-\overline{s}}{3}\left(\frac{\sin\phi}{\overline{s}}\right)^{2}\left(1+3\overline{s}-\left(\frac{s}{\overline{s}}\right)^{-\frac{3}{2}}\right)s \qquad (84)$$

$$K=\lim_{s\to0}\frac{\chi_{x}^{e}}{\chi_{z}^{e}}=-\infty \qquad (85)$$

Note: K is undefined because χ_{z}^{e} is undefined at s=0.

Case (4): $r(\eta,1/2,1)=1-\left(1-\eta\right)^{1/2}$

$$\chi_{xz}^{e}=\left(1-\left(1-\frac{s}{\overline{s}}\right)^{\frac{1}{2}}\right)\overline{\chi}_{xz},\ \frac{\partial\chi_{xz}^{e}}{\partial s}=\left(1-\frac{s}{\overline{s}}\right)^{\frac{-1}{2}}\frac{\overline{\chi}_{xz}}{2\overline{s}} \qquad (86),\ (87)$$

$$\chi_{x}^{e}=\left(1-\overline{s}\right)\left(1-s+\left(1+\frac{4-s/\overline{s}}{3}\sqrt{1-s/\overline{s}}\right)\overline{s}\right)\cos^{2}\phi \qquad (88)$$

$$\chi_{z}^{e}=1-s+\frac{s\left(1-\overline{s}\right)}{\overline{s}\csc^{2}\phi}\left(1-\frac{\sqrt{1-\frac{s}{\overline{s}}}}{2s}-\frac{\tanh^{-1}\sqrt{1-\frac{s}{\overline{s}}}}{2\overline{s}}\right) \qquad (89)$$

$$K=\lim_{s\to0}\frac{\chi_{x}^{e}}{\chi_{z}^{e}}=\frac{2\left(1-\frac{\overline{s}}{3}\right)\left(1-\overline{s}\right)\overline{s}\cos^{2}\phi}{2\overline{s}-\left(1-\overline{s}\right)\sin^{2}\phi} \qquad (90)$$

Case (5): $r(\eta,2,1)=1-\left(1-\eta\right)^{2}$

$$\chi_{xz}^{e}=\left(1-\left(1-s/\overline{s}\right)^{2}\right)\overline{\chi}_{xz},\ \frac{\partial\chi_{xz}^{e}}{\partial s}=2\left(1-\frac{s}{\overline{s}}\right)\frac{\overline{\chi}_{xz}}{\overline{s}} \qquad (91),\ (92)$$

$$\chi_{x}^{e}=\left(1-\overline{s}\right)\left(1+\left(1-\left(s/\overline{s}\right)^{3}\right)\frac{\overline{s}}{3}\right)\cos^{2}\phi \qquad (93)$$

$$\chi_{z}^{e}=1-s-2\left(1-\overline{s}\right)\left(\frac{\sin\phi}{\overline{s}}\right)^{2}\left(1-\left(1+\frac{\overline{s}}{2}-\ln\left(\frac{s}{\overline{s}}\right)\right)s\right) \qquad (94)$$

$$K=\lim_{s\to0}\frac{\chi_{x}^{e}}{\chi_{z}^{e}}=\frac{\left(1+\frac{\overline{s}}{3}\right)\left(1-\overline{s}\right)\overline{s}\cos^{2}\phi}{\overline{s}-2\left(1-\overline{s}\right)\sin^{2}\phi} \qquad (95)$$

References

1) Jáky, J., A nyugalmi nyomâs tényezöje (The coefficient of earth pressure at rest), *Magyar Mérnok és Epitész Egylet Közlönye (Journal for Society of Hungarian Architects and Engineers)*, Vol.7, pp.355-358, 1944
2) Jáky, J., Earth pressure in silos. *Proceedings of the 2nd International Conference on Soil Mechanics and Foundation Engineering-ICSMFE*, London, Vol.1, pp.103-107, 1948
3) Kenney, TC, Discussion on "Geotechnical properties of glacial lake clays" by Wu, T.H. (1958), *ASCE-Journal of Soil Mechanics and Foundations Engineering Division*, Vol.85, No.SM3, pp. 67-79, 1959
4) Brooker, E.W. and Ireland, H.O., Earth pressures at rest related to stress history, *Canadian Geotechnical Journal*, Vol.2, No.1, pp.1-15, 1965
5) Mayne, P.W. and Kulhawy, F.H., K_o-OCR relationships in soil, *Journal of the Geotechnical Engineering Division-ASCE*, Vol.108, No.6, pp.851-872, 1982
6) Mesri, G. and Hayat, T.M., The coefficient of earth pressure at rest, *Canadian Geotechnical Journal,* Vol.30, No.4, pp.647-666, 1993
7) Watabe, Y., Tanaka, M., Tanaka, H. and Tsuchida, T., K_0-consolidation in a triaxial cell and evaluation of in-situ K_0 for marine clays with various characteristics, *Soils and Foundations*, Vol.43, No.1, pp.1-20, 2003
8) Tschebetarioff, G., *Soil Mechanics, Foundations, and Earth Structures*, McGraw-Hill, New York, pp.254-256, 1951
9) Handy, R.L., The arch in soil arching, *ASCE-Journal of Geotechnical Engineering,* Vol. 111(3), pp.302-318, 1985
10) Michalowski, R.L. and Park, N., Admissible stress fields and arching in piles of sand, *Geotechnique*, Vol.54(8), pp.529-538, 2004
11) Michalowski, R.L., Coefficient of earth pressure at rest, *Journal of Geotechnical and Geoenvironmental Engineering-ASCE*, Vol.131, No.11, pp.1429-1433, 2005
12) Brahtz, J.H.A., Rational Design of Earth Dams, *Transactions of the 2nd International Congress on Large Dams,* Washington D.C., Vol.4, pp. 543-576, 1936
13) Vanel, L., Howell, D., Clark, D., Behringer, R.P. and Clement, E., Memories in sand: Experimental tests of construction history on stress distributions under sandpiles, *Physical Review E*, Vol.60(5), pp.R5040-R5043, 1999
14) Wittmer, J. P., Claudin, P., Cates, M. E. and Bouchaud, J. P., An explanation for the central stress minimum in sand piles, *Nature*, Vol.382, No.6589, pp.336-338, 1996
15) Wittmer, J.P., Cates, M.E. and Claudin, P., Stress propagation and arching in static sandpiles, *Journal De Physique I*, Vol.7, No. 1, pp.39-80, 1997
16) Cantelaube, F. and Goddard, J.D., Elastoplastic arching in 2D granular heaps, *Powders & Grains 97,* pp.231-234, 1997
17) Cates, M.E., Wittmer, J.P., Bouchaud, J.P. and Claudin, P., Development of stresses in cohesionless poured sand, *Philosophical Transactions of the Royal Society of London Series a-Mathematical Physical and Engineering Sciences*, Vol.356, No.1747, pp.2535-2560, 1998
18) Didwania, A.K., Cantelaube, F., and Goddard, J.D., Static multiplicity of stress states in granular heaps, *Proceedings of the Royal Society of London Series a-Mathematical Physical and Engineering Sciences*, Vol.456(2003), pp. 2569-2588, 2000
19) Krynine, D.P., Discussion: Stability and stiffness of cellular cofferdams by Karl Terzaghi, *Transactions-ASCE*, Vol.110, pp.1175-1178, 1945
20) Heng, S., Pipatpongsa, T. and Ohta, H., Jáky's inconsistent assumptions on stress analyses in sand heap and storage silo, *Geo-Kanto*, Tokyo, pp.331-336, 2008
21) Savage, S. B., Modeling and granular material boundary values problems, *Physics of dry granular media*, Kluwer Academic Press, NATO ASI Series E 350, pp.25-94, 1998
22) Trollope, D.H., The systematic arching theory applied to the stability analysis of embankments, *Proceedings of the 4th International Conference on Soil Mechanics and Foundation Engineering*, 1957
23) Trollope, D.H. and Burman, B.C., Physical and numerical experiments with granular wedges, Geotechnique, Vol.30, No.2, pp.137-157, 1980
24) Sokolovskii, V.V., *Statics of Granular Materials*, English translation edition, Pergamon Press, pp.219-236, 1965
25) Tejchman, J. and Wu W., FE-calculations of stress distribution under prismatic and conical sandpiles within hypoplasticity, *Granular Matter*, 10(5), pp. 399-405, 2008
26) Hummel, F.H. and Finnan, E.J., The distribution of pressure on surfaces supporting a mass of granular material, *Minutes of Proc., Institute of Civil Engineering*, Session 1920-1921, Part II, Selected papers 212, pp.369-392, 1920
27) Lee, I.K. and Herington, J.R., Stress beneath granular embankments, *Proceedings of the First Australia-New Zealand Conference on Geomechanics*, Melbourne, pp. 291-297, 1971
28) Bouchaud, J.P., Cates, M.E. and Claudin, P., Stress-distribution in granular media and nonlinear-wave equation, *Journal De Physique I*, Vol.5(6), pp.639-656, 1995
29) Pipatpongsa, T., Tachibana, S. and Ohta, H., Statics of granular media in wedge-shaped mound, *Geo-Chiangmai*, Chiangmai, pp.269-274, 2008

(Received: April 9, 2009)